Chapter 7

BIFURCATION THEORY, SYMMETRY BREAKING AND HOMOGENIZATION IN CONTINUUM MECHANICS DESCRIPTIONS OF DNA

Mathematical Modelling of the Physics of the Double Helix

John H. Maddocks
Bernoulli Mathematics Institute
Swiss Federal Institute of Technology–Lausanne
CH-1015 Ecublens
John.Maddocks@epfl.ch

Abstract The study of DNA minicircles, i.e. closed loops of the double helix with lengths of the order of a few hundred base pairs, is a commonly used experimental technique to probe the sequence-dependent mechanical properties of DNA, such as stiffnesses and intrinsic shape. This article reviews how the mathematical methods of bifurcation theory and symmetry breaking can be used to compute the sequence-dependent equilibrium shapes of mini-circles. The computations yield quite good comparison with experimental data, despite the fact that they assume an isotropic bending law for the DNA, and that at the single base-pair scale the bending response of DNA is almost certainly strongly anisotropic. The effective isotropic behavior can be explained via a two-scale expansion involving the high intrinsic twist parameter of the DNA double helix (one turn per 10.5 base pairs). The effective isotropic stiffnesses can be found in terms of the local anisotropic stiffnesses via a study of the lowest order term in this expansion. However to understand the first correction, symmetry breaking techniques are again required.

Keywords: DNA minicircles, elastic rods, cyclization, Poincaré-Melnikov functions, continuous symmetry, isotropy

Introduction

Arguably the two greatest scientific achievements of the first half of the 20th century were the theories of relativity and of quantum mechanics. Similarly a good case can be made that the two most significant scientific developments of the second half of that century were the development and exploitation of computers, and the establishment of the discipline of molecular biology, as was largely catalyzed by the 1953 discovery by Watson and Crick of the DNA double helix secondary structure. (The original reference is [1], which is reprinted along with several other related articles in [2].)

One of the goals of this volume is to celebrate the scientific applications of mathematics and mathematical modelling. The fundamental role of mathematics in the theories of relativity and quantum mechanics, where it provides the basic language, seems self-evident. In computation, mathematics and mathematical modelling are essential to the construction of both hardware and algorithms, while, contrariwise, the widespread availability of higher and higher performance scientific computing has fundamentally altered the mathematical landscape, with vastly increased importance for the domain of numerical analysis, and a complete redefinition of what can be regarded as a useful and tractable mathematical model.

The case for the influence of mathematics on the development of molecular biology during the 20th century is less compelling[1]. There are some interesting mathematical stories to tell, for example knot theory combined with electron microscope observations of knot types of closed loops of the DNA double helix has been used to probe the actions of DNA cutting enzymes (an introduction to the background of this and several other topics mentioned in this article can be found in the monograph [4] or the review [5]). And the Călugăreanu-Fuller-White formula $Lk = Tw + Wr$ [6, 7, 8, 9, 10, 11], relating the Link, Twist and Writhe of a closed ribbon—a topological formula with a certain nontrivial mathematical sophistication—is now so widely used to explain the supercoiling of DNA that it appears in introductory biochemistry textbooks [12]. But these anecdotes are completely overshadowed by what will in due course presumably be considered as one of the greatest scientific achievements of the 21st century, namely the publication of the human genome [13].

[1]For example there is a famous 1953 image of Crick and Watson standing beside the original, and truly physical, model of DNA for which the caption appearing in [3] runs ' .... For purposes of the picture Crick was persuaded to point with a slide rule even though he had not used one in preparing the model.'

The human and other genomes are a complete listing of the primary structure of the DNA in an organism, namely the complete ordered list of the four bases A, T, C and G. In the case of humans this means 3.2 billion or so occurrences of the letters. The sequencing of entire genomes is a triumph of automated biochemistry achieved by building robots that determine the sequence of fragments of DNA, combined with extensive computation to identify overlaps between sequence fragments to assemble the whole. This is the stuff of classic bioinformatics—the assembly of huge databases of biomolecular sequence information through the exploitation of a combination of the two 20th century (and at that time completely independent) scientific breakthroughs of scientific computing and molecular biology. The contributions of mathematics and statistics to the genome projects, and bioinformatics more generally, has already been vast, but has so far largely involved what might be described as discrete mathematics and statistics, pattern matching etc.

A second goal of this volume is to celebrate the myriad mathematical contributions of Joseph B. Keller (hereafter and forevermore JBK). To my (albeit highly limited) knowledge, JBK has not published in the field of relativity (at least not yet). He certainly has contributed to the development of quantum mechanics via semi-classical methods (see e.g. [14]). His contributions to the field of scientific computing are profound and extensive via his development of asymptotic methods and the construction of simplified mathematical models of physical systems that just happen to capture the essence of the problem. While he has published widely in several areas of mathematical biology and mathematical medicine, he has not (again to my limited knowledge) worked directly in molecular biology.

The goal of this Introduction is to make the claim that the influence of JBK on molecular biology is just beginning, and that it will also be profound. In the particular case of DNA, much is known concerning which parts of the genome are responsible for which functions, and which changes will lead to which diseases. But this knowledge is largely phenomenological. Comparatively little is known of the detailed physical mechanisms by which DNA functions. What are the particular properties of a sequence which mean that transcription is initiated there, in such and such circumstances, and what is the physical mechanism? How is the DNA packed and unpacked? Understanding such questions requires physical, and frequently stochastic, modelling of the type in which JBK excels. Such models involve mathematics of a completely different character than has thus far been extensively exploited in the disciplines of bioinformatics, biocomputing and biosimulation. DNA represents only one example of a molecular or cell biology system which seems likely to benefit from the development of physical models with a continuum mechanics flavor; other examples include actin and collagen filaments, microtubules, lipid bilayers, and molecular motors. The widespread study of such systems is just starting to be pursued by a number of applied mathematicians, many of whom JBK helped to train directly, or mathematically grandfathered or great-grandfathered as PhD students or postdocs, and the techniques being exploited involve many of the (by now basic) methods of applied mathematics that JBK helped to develop. For example the Stokes flow slender body theory developed in [15] (and originally motivated by [16]) seems quite likely to have a role to play in modelling the mobility of DNA molecules in gels, a problem which is starting to attract the attention of mathematicians, e.g. [17].

The goal of this article is to give one example of how classic applied mathematics techniques can be used in molecular biology. In particular I will present an overview of work by my collaborators and myself in the specific context of modelling DNA, which I hope illustrates the way in which bifurcation theory, asymptotic expansions, multiple-scales and symmetry breaking can make some contribution to the understanding of how DNA functions. The mathematical presentation is based primarily on [18, 19, 20], but also draws on material from [21, 22, 23, 24, 25, 26].

1. So what is DNA?

The ordered list or base-pair sequence appearing in a genome is the primary structure of the DNA. Each of the four bases A, C, G, and T has a known atomistic structure. The Nobel prize winning observation of Watson and Crick was that the bases A and T and C and G could be paired in such a way that the stereo-chemistry (or three dimensional geometry) of each base pair AT or CG was essentially identical, and the base-pairs could be linked with sugar-phosphate chains and assembled into a right-handed double helix with an arbitrary sequence of bases along one backbone, and the complementary sequence along the other, cf. Figures 7.1a and 7.1b. While each base-pair is of very similar geometry, each pair is formed from one smaller base (a pyrimidine, C or T) and one larger base (a purine, A or G). Moreover, the AT base pairing has two hydrogen bonds, while the CG pair has three. Due to these and other differences, and therefore dependent upon the sequence, it is believed that the geometry of the backbones deviates from that of an ideal circular helix, and the physical properties such as stiffness vary along the molecule. Further than that, in some circumstances double stranded DNA can be, in continuum mechanics terms, a multi-phase molecule; the bases can be paired in different, sometimes drastically different, ways to form a variety of helical structures, but the standard, most usual one is called B-form. Describing transitions between the possible forms is an important issue, but appropriate mathematical models are beyond the scope of this overview.

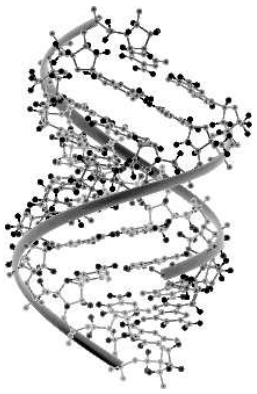

Figure 7.1a. A computer simulation at atomic resolution of a short segment of the DNA double helix. The base pairs form in the interior, while the sugar-phosphate backbones form the double helix. The diameter of the double helix is approximately 2 nanometers, with a complete helical turn every 10.5 base pairs or 3.5 nanometers.

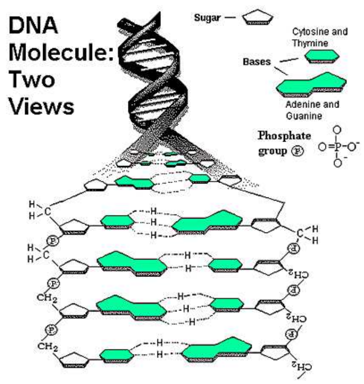

Figure 7.1b. A cartoon of the DNA secondary structure. The chemistry of the backbones is such that they have an orientation, which is anti-parallel in standard DNA. The bases have different sizes, and the base pairings are formed with either two or three hydrogen bonds.

In genes (or coding regions) the primary role of the primary structure (or sequence) of DNA is to code for which proteins are produced when the gene is expressed. But in the human genome the currently known coding regions make up only 2% or so of the whole, so what, if anything, does the rest of the DNA do? As there are approximately 3.2 billion base pairs in the human genome, and the helical rise of each base pair is approximately 0.34 nanometers, a rather attractive cancellation of exponents of ten reveals that the arc-length of the human DNA present in each cell of our body is approximately 1 meter. (Chapter 1 of the introductory text [27] has a number of such computations related to the scales of DNA.) Clearly the DNA is stored in a highly compacted, and organized way that allows cell division, and the expression of the right genes in the appropriate parts of bodies at the right times in our lives. This mechanism of storage is an extremely complicated thing which certainly operates on a hierarchy of scales and which involves interactions between DNA and a number of different proteins. Nevertheless there is a general conjecture that the sequence-dependent mechanical properties of DNA at the scale of a few hundred base pairs and below plays a crucial role in how DNA functions.

Why is the scale of a few hundred base pairs special? In physical terms DNA is a heteropolymer—each mer is a base-pair but the mers vary along the chain. In the standard statistical mechanics theory of homopolymers one of the most important concepts is that of *persistence length*. In a standard Gaussian model of an intrinsically straight homopolymer in a solvent, it can be calculated that the correlation between tangent vectors at two points along the polymer decays exponentially with the difference in arc-length between the points, and the length scale of this decay is the persistence length. The story for DNA is more complicated [28] because DNA is usually neither intrinsically straight, nor a homopolymer, but the persistence length is nevertheless accepted to be of the order of 150 base pairs or so. For our purposes this scale indicates that in solution the sequence-dependent elastic properties will have significant effects on the physical behavior of DNA fragments, or oligomers, shorter than two or three hundred base pairs, while for longer segments of DNA, entropic effects, which are largely sequence independent, will gradually dominate.

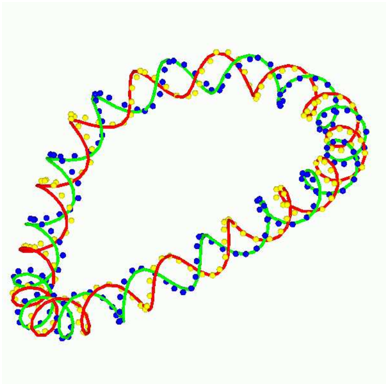

Figure 7.2. A configuration of a minicircle in both the rigid base-pair (dots) and continuum (lines) descriptions.

Minicircles are closed loops of DNA [5] in which the double helix bends around to close on its own tail with some number of twists, cf. Figure 7.2. By a variety of biochemical methods the same oligomer can often be formed into different topoisomers, i.e. the minicircle can be closed with a different number of imposed twists, or equivalently with different links of the two backbones. Such minicircles provide a very attractive experimental motif within which the mechanics of DNA can be studied because the molecule is stressed, with different loadings for different topoisomers, without there being any difficulties associated with end-effects or external loading devices. The three-dimensional shapes of minicircles can be observed directly via the technique of cryo-electron-microscopy [5, 29, 30], although they are close to the shortest molecules that can be resolved, and the development of a quantitative estimate of the error in shape reconstruction from cryo-EM images of DNA minicircles is a current research topic.

An alternative experimental technique involving minicircles is to measure relative cyclization rates, i.e. the rates of formation of minicircles, of oligomers with different base-pair sequences. Indeed the first sentence of the abstract of [31] reads *'DNA cyclization is potentially the most powerful approach for systematic quantification of sequence-dependent DNA bending and flexibility'.* According to statistical mechanics a first approximation to the cyclization rate of a given minicircle is provided by the potential energy of the closed, local minimizer of that link. And, in a mathematical paraphrase of the idea proposed in [31], corrections to the cyclization rate can be had by study of the second variation around a given minimizer (i.e. in the harmonic approximation about each energy well).

The remainder of this article describes how to compute the cyclized shapes and energies of minicircles that realize local minimizers of the potential energy, assuming that the parameters of the appropriate potential energy are known. In fact the determination of accurate constitutive relations for DNA at the levels of atomistic, base, base-pair and continuum descriptions is an active, difficult, and ongoing research area both within my, and several other, groups throughout the world [32, 33, 34, 35, 36]. However in order to focus on the mathematical modelling and computational techniques, we shall assume that appropriate constitutive relations are given. Moreover, we shall not assume the most general possible constitutive relations, but rather concentrate on the simplest possible cases that illustrate the underlying mathematical ideas, namely those where extension and shear between base-pairs is negligible, and the energy of bending and twist is quadratic and diagonal (in a sense to be made more precise below). Nevertheless it is important to understand that the usefulness of the mathematical techniques to be described in no way depends upon these simplifying assumptions; rather they carry over to the most general cases, but with more complications in the detailed calculations required. In fact the main motivation for the development of the mathematical methods is to provide a route to extract predictions from a given set of constitutive relations at scales that can be checked directly against independent experimental observables.

2. Cosserat rods and the Hamiltonian form of the equilibrium conditions

We begin by summarizing the special Cosserat theory (see, e.g. [37]), which is commonly used in continuum mechanics to model an inextensible and unshearable rod, or an *elastica.* The configuration of a rod is specified by two smooth vector-valued functions (cf. Figure 7.3a)

$$\mathbf{r}(s), \mathbf{d}_1(s) : [0,1] \to \mathbb{R}^3.$$

In the context of DNA, the curve $\mathbf{r}(s)$ can be interpreted as the centerline of the double helix, with $\mathbf{d}_1(s)$ being a unit vector normal to the centerline that serves to locate the orientation of the backbones. We assume that for the loadings of concern the DNA is effectively unshearable and inextensible. Mathematically, unshearability and inextensibility are expressed by setting $\mathbf{r}' = \mathbf{d}_3$ with $\mathbf{d}_3 \cdot \mathbf{d}_1 = 0$, and defining $\mathbf{d}_2 = \mathbf{d}_3 \times \mathbf{d}_1$ to obtain a right-handed orthonormal frame $\{\mathbf{d}_i\}_{i=1}^3$, called the *directors.* With the assumption of inextensibility the parameter $s \in [0,1]$ can be interpreted as nondimensionalized arclength in any configuration of the DNA molecule.

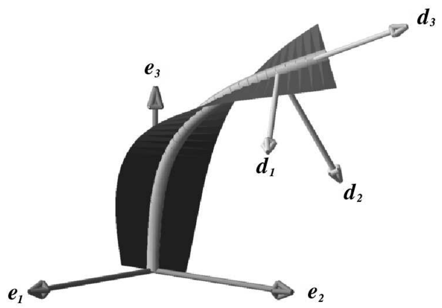

Figure 7.3a. A configuration of an elastic rod. The tube represents the centerline $\mathbf{r}(s)$. The triad $\{\mathbf{d}_i(s)\}$ indicates the orientation of the cross-section, with $\mathbf{d}_1$ generating the ribbon that visualizes twist.

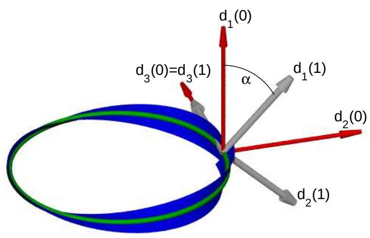

Figure 7.3b. The twisted ring boundary value problem: the centerline $\mathbf{r}(s)$ is constrained to form a smoothly closed loop, while a twist angle α is imposed between the directors $\mathbf{d}_1(0)$ and $\mathbf{d}_1(1)$.

Orthonormality of the directors $\{\mathbf{d}_i\}$ implies the existence of a *strain vector* $\mathbf{u}$ satisfying

$$\mathbf{d}_i' = \mathbf{u} \times \mathbf{d}_i, \quad i = 1, 2, 3. \tag{7.1}$$

The components $u_i = \mathbf{u} \cdot \mathbf{d}_i$ with respect to the frame $\{\mathbf{d}_i\}$ are the bending ($i = 1, 2$) and twisting ($i = 3$) strains. We gather the three components u_i in a triple u.

In rod mechanics the forces and moments acting across a material cross-section are averaged into a net force $\mathbf{n}(s)$ and a net moment $\mathbf{m}(s)$. Then balance of moments and forces imply the coordinate free equilibrium equations

$$\mathbf{m}' + \mathbf{r}' \times \mathbf{n} = \mathbf{0}, \quad \mathbf{n}' = \mathbf{0}. \tag{7.2}$$

The components $m_i = \mathbf{m} \cdot \mathbf{d}_i$ are the bending and twisting moments in the rod. As above, the triple of director components (m_1, m_2, m_3) is denoted m.

The moments m_i must be related to the strains u_i via suitable constitutive relations. We make the assumption of hyperelasticity: for $\mathsf{v} = (\mathsf{v}_1, \mathsf{v}_2, \mathsf{v}_3)$ there exists a convex strain energy density function $W(\mathsf{v}, \mathsf{s})$ such that $W_{\mathsf{v}}(\mathbf{0}, \mathsf{s}) = \mathbf{0}$, and the constitutive relations are of the form $m_i = W_{v_i}(\mathsf{u} - \hat{\mathsf{u}}, \mathsf{s})$. Here $\hat{\mathsf{u}}(s) = (\hat{u_1}(s), \hat{u_2}(s), \hat{u_3}(s))$ are the components of strain in the minimum energy unstressed configuration. Our results will be particularly explicit when the strain energy density function is assumed to be of the standard diagonal quadratic form

$$W(\mathsf{v}, \mathsf{s}) = \frac{1}{2} \sum_{\mathsf{i}=1}^{3} \mathsf{K}_{\mathsf{i}}(\mathsf{s}) \mathsf{v}_{\mathsf{i}}^2, \tag{7.3}$$

which generates decoupled linear constitutive relations

$$m_i = K_i(u_i - \hat{u}_i). \tag{7.4}$$

Then $K_1(s)$ and $K_2(s)$ are called the bending stiffnesses, and $K_3(s)$ is the twist stiffness. In the context of DNA the implicit s dependence of the strain energy density function through the $\hat{u}_i(s)$ parameters encodes the sequence-dependence of the shape of the oligomer in its minimal potential energy configuration. The explicit s dependence of the strain energy density function (the $K_i(s)$ in the quadratic case) models the sequence dependent variations in the stiffness of the oligomer.

With the above assumptions and notation, and after suitable nondimensionalization, the equilibrium configurations of a rod are critical, or stationary, points of the potential energy

$$\int_0^1 W(\mathsf{u} - \hat{\mathsf{u}}, \mathsf{s}) - \mathbf{n} \cdot \mathbf{d}_3 \, \mathsf{ds}, \tag{7.5}$$

subject to appropriate side and boundary conditions. The linear term in $\mathbf{n}$ appearing in the potential energy arises from the assumption of inextensibility and unshearability; one valid interpretation is to regard $\mathbf{n}$ as a (constant) triple of associated Lagrange multipliers. As previously remarked, finding the local minimizers and other critical points of the potential energy (7.5) is a first step toward understanding the statistical mechanical probability distribution of a rod (the DNA) immersed in a solvent.

Finding critical points of the energy (7.5) is a problem of the one-dimensional calculus of variations. The only slightly non-standard aspects are that the variational principle involves taking variations which respect the inextensibility and unshearability condition, and which (because of the presence of the orthonormal directors amongst the configuration variables) respect the geometry of $SO(3)$ i.e. the group of proper rotations.

Appropriate treatment of $SO(3)$ is a standard issue in continuum mechanics that can be handled in variety of ways, either picking coordinates on $SO(3)$, or adopting an intrinsic formulation of the variations. In either case the first-order necessary conditions, or Euler-Lagrange equations, that must be satisfied by stationary points can be shown (see [24] for example) to have a Hamiltonian form

$$\mathbf{z}' = \mathbf{J}\nabla H(\mathbf{z}, s) \tag{7.6}$$

with associated Hamiltonian

$$H(\mathbf{z}, s) = W^*(\mathsf{m}, \mathsf{s}) + \mathsf{m} \cdot \hat{\mathsf{u}}(\mathsf{s}) + \mathbf{n} \cdot \mathbf{d}_3, \tag{7.7}$$

where $W^*(\mathsf{m}, \mathsf{s})$ is the Legendre transform of the given strain energy density function $W(\mathsf{v}, \mathsf{s})$. The Legendre transform corresponding to the specific quadratic strain energy function (7.3) is

$$W^*(\mathsf{m}, \mathsf{s}) = \frac{1}{2}\sum_{\mathsf{i}=1}^{3} \mathsf{K_i}(\mathsf{s})^{-1}\mathsf{m}_\mathsf{i}^2. \tag{7.8}$$

The notation in (7.6) and (7.7) has deliberately been left somewhat imprecise. In fact there are several equivalent Hamiltonian systems dependent upon the precise form taken for the independent variable $\mathbf{z}$, and the way that is chosen to handle $SO(3)$ [24].

Working with some Hamiltonian form of the equilibrium conditions is desirable for a variety of reasons. For example the effects of continuous symmetries are easily handled, and the differential equations are first-order in space. All of the Hamiltonian forms are equivalent in that they generate the appropriate equilibrium conditions (7.2), and all of the formulations have (7.20) as Hamiltonian, although the variables m may themselves be functions of the chosen phase variable $\mathbf{z}$. The form of the skew-symmetric matrix $\mathbf{J}$ is perhaps the most significant difference between formulations. For the homogenization results to be described later, we further need that $\mathbf{J}$ takes the canonical symplectic form

$$\mathbf{J} = \begin{pmatrix} \mathbf{0} & \mathbf{I} \\ -\mathbf{I} & \mathbf{0} \end{pmatrix}, \tag{7.9}$$

because canonical changes of variable play a central role in the analysis developed in [20, 23]. The matrix $\mathbf{J}$ does take the form (7.9) if explicit coordinates are chosen on $SO(3)$. In my group's work we have found it particularly convenient to adopt the quaternion, or Euler parameter, description of $SO(3)$, as is frequently done in many fields of application, including computational chemistry. However there are some delicate points in deriving the associated *Hamiltonian* form, and I am unaware of any Hamiltonian formulation involving quaternions prior to the description given in [21].

3. The integrable, symmetric case

One advantage of adopting the Hamiltonian form (7.6) is that one has access to the machinery of complete integrability and continuous symmetries. The rod equilibrium equations are completely integrable when the Hamiltonian (7.7) has the two continuous symmetries of being uniform (or autonomous) and being transversely isotropic.

Uniformity corresponds to the absence of explicit s-dependence in the strain energy function W and in the shape parameters $\hat{\mathsf{u}}$. For uniform rods the Hamiltonian is constant as a function of s along equilibria. The discussion given here will not focus on the ramifications of this symmetry. In contrast the notion of transverse isotropy (usually shortened to isotropy) will play an important role in the presentation. The strain energy function is isotropic if

$$W(\kappa\cos\theta, \kappa\sin\theta, v_3, s) \quad \text{is independent of } \theta \tag{7.10}$$

for all κ, v_3, and s. For the quadratic energy (7.3) isotropy is equivalent to $K_1(s) \equiv K_2(s)$. The rod will be called isotropic if in addition the intrinsic curvatures vanish, $\hat{u}_1(s) \equiv \hat{u}_2(s) \equiv 0$. Isotropic rods are those for which the twist moment m_3 is constant along equilibria.

It is simple to demonstrate that W is uniform and isotropic precisely if the Legendre transform W^* is uniform and isotropic. Accordingly the integrable version of the Hamiltonian(7.7) is[2]

$$H(\mathbf{z}) = W^*(\mathsf{m}) + \mathsf{m}_3\hat{\mathsf{u}}_3 + \mathbf{n}\cdot\mathbf{d}_3, \tag{7.11}$$

with $W^*(\kappa\cos\theta, \kappa\sin\theta, v_3)$ being independent of θ.

The continuous symmetries which generate integrals also generate special solutions. For the integrable Hamiltonian (7.11) it is a classic result that uniformly twisted rods with a circular centerline are equilibria [38, 39, 40, 41][3]. Moreover all solutions, not just these special ones, are *non-isolated* solutions of the twisted ring two-point boundary value problem illustrated in Figure 7.3b. The non-isolation is due to the symmetry of isotropy as explained in Figure 7.4 and the transformation rule

Register Transformation For $0 \le \theta < 2\pi$,

Step 1: Rotate the ring rigidly by an angle θ about the z axis.

Step 2: Locally rotate the rod about its tangent vector $\mathbf{r}'$ by $-\theta$.

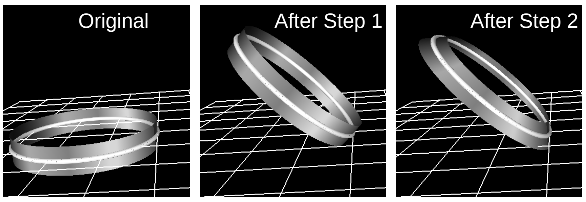

Figure 7.4. Register Symmetry: The original solution and its images after Steps 1 and 2 of the register transformation for $\theta = 45°$. The z axis lies on the grid, pointing away from the viewer.

Note that this register transformation respects boundary conditions, and so generates a family of solutions of the boundary value problem, and not just of the field equations. In particular, the register symmetry couples the material symmetry of isotropy with the rigid body symmetry of rotation in space to ensure that both the differential equations and boundary conditions are satisfied. A similar argument carries through for the symmetry of translation in arc-length, but for reasons of space we will not discuss it here, see [22].

4. Symmetry breaking

The explicit twisted circle solutions to the integrable problem serve as starting points for a numerical computation, via parameter continu-

[2]In point of fact if the rod is isotropic one can allow s dependence in $\hat{\mathsf{u}}_3(s)$ for example, and still retain complete integrability, but this is a fine detail.
[3]With thanks to A. Goriely for providing the citation [38].

ation, of the entire connected component of solutions, cf. Figure 7.5a. The next step is to perturb from this integrable *perfect problem* with $\hat{u}_i(s) \equiv 0$ to other *imperfect problems* with small, but nonzero, intrinsic curvatures $\hat{u}_i(s)$, and with the same constitutive functions W (or equivalently the same W^*). In [18] this process was analyzed as a (regular) asymptotic expansion. The only issue of note is that as all solutions to the non-perturbed problem are non-isolated, the linear operator arising in the expansion necessarily has null space (containing the tangent vectors to the symmetry orbit), so that solvability conditions arise in the inhomogeneous, linear systems in the expansion. These solvability conditions select certain isolated members of the symmetry related family of solutions to the unperturbed problem as being the only ones that persist through the symmetry breaking. Typical results are shown in Figure 7.5b.

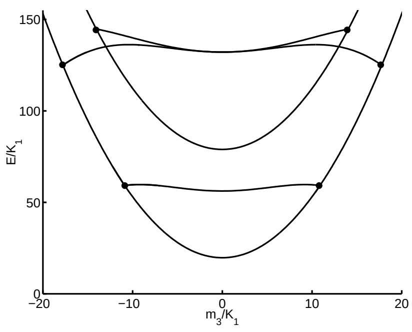

Figure 7.5a. A bifurcation diagram for the perfect problem. As the twist parameter α is varied, the energy E and twist moment m_3 of the ring equilibria are plotted. The parabolic (*trivial*) branches correspond to loops of planar equilibria with circular centerlines generated by the register symmetry, while the remaining (*nontrivial*) branches correspond to tori of nonplanar equilibria. (In both parts a) and b) only points marked with a dot correspond to bifurcation points, other crossings result from the projection to two dimensions.)

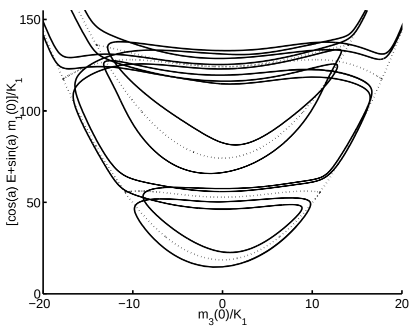

Figure 7.5b. A bifurcation diagram (solid line) with perturbed intrinsic curvatures. The perfect bifurcation diagram from part a) is included for comparison (dotted line). The trivial branches representing loops of solutions in part a) have degenerated into two branches each representing equilibria that are locally isolated (at fixed α). Similarly, nontrivial branches representing tori of solutions have split into four branches of isolated equilibria.

The analysis subsequently developed in [20] allows the conclusions of [18] to be summarized more succinctly within a more general framework. Specifically, consider parameter dependent, Hamiltonian systems of the form

$$\mathbf{z}' = \mathbf{J}\nabla H(\mathbf{z}, s; \epsilon)\,, \tag{7.12}$$

subject to appropriate two-point boundary conditions (that are associated with an action principle) on the unknown $\mathbf{z}(s;\epsilon)$. Assume further that for the unperturbed $\epsilon = 0$ problem there is a (for simplicity one-dimensional) symmetry-related family of equilibria $\mathbf{z}^{\theta}(s)$, where θ parameterizes the family. Then the members $\mathbf{z}^{\theta^*}(s)$ of this family that can be ϵ-limits of branches of solutions $\mathbf{z}(s;\epsilon)$ to (7.12) are critical points of the Poincaré function

$$P(\theta) \equiv \int_0^1 H_\epsilon(\mathbf{z}^{\theta}(s), s; 0)\, ds\,, \tag{7.13}$$

where H_ϵ denotes partial derivative. In other words the Poincaré function is the first-order ϵ perturbation of the Hamiltonian evaluated on the orbit of the symmetry related solutions to the unperturbed $\epsilon = 0$ problem. The derivative $P_\theta(\theta)$ is the Melnikov function for the system (7.12). In the case of the register transformation the symmetry orbit is topologically a circle and consequently the Poincaré function always has at least two critical points, namely a maximum and a minimum, and generically that is all. Thus it can be anticipated that of the loop of twisted circle equilibria only two will persist, and this is what is typically observed.

Contrariwise in [20] it is demonstrated that with mild regularity assumptions, the methods of [42] or [43] can be adapted for the Cosserat rod problem to conclude that any solution $\mathbf{z}^{\theta^*}(s)$ that is a non-degenerate critical point of (7.13) (respectively a simple root of the Melnikov function) can be embedded in a family of solutions $\mathbf{z}(s;\epsilon)$ of the perturbed problem.

5. Applications to DNA minicircles

A numerical version of the symmetry breaking approach outlined in the previous Section was already exploited in [22] to compute energies of cyclized DNA minicircle equilibria (such as that depicted in Figure 7.2), and the results gave favorable comparison with cyclization experiments. The point is that the only delicate step in the computations is to continue to small non-vanishing shape parameters. Once the symmetries have been broken, the numerical continuation to large intrinsic shape parameters appropriate for DNA is straightforward, and bifurcation diagrams of the qualitative form depicted in Figure 7.5b are found. Only certain points on this diagram correspond to closed framings, and it is these configurations that yield the predictions for minicircle energies and shapes that are compared with experiment.

The insights of the perturbation analysis of [18] were also used in [26] to identify DNA oligomer sequences that should cyclize atypically, and which are therefore good candidates for experiments aimed at testing the accuracy of the assumed constitutive relations.

It is now time to address the implicit assumption that the configurations of DNA minicircles can be computed by using the case of an integrable rod as an organizing center. This is a reasonable presumption if the limit of vanishing intrinsic curvature yields an isotropic rod. In turn that will be the case if the strain energy density function W is itself isotropic. But as remarked in the abstract, the bending stiffnesses of DNA at the base-pair scale are almost certainly rather anisotropic, because of the rectangular shape of base pairs that is illustrated in Figure 7.1b. The missing ingredient that remains to be discussed is the high intrinsic twist of DNA.

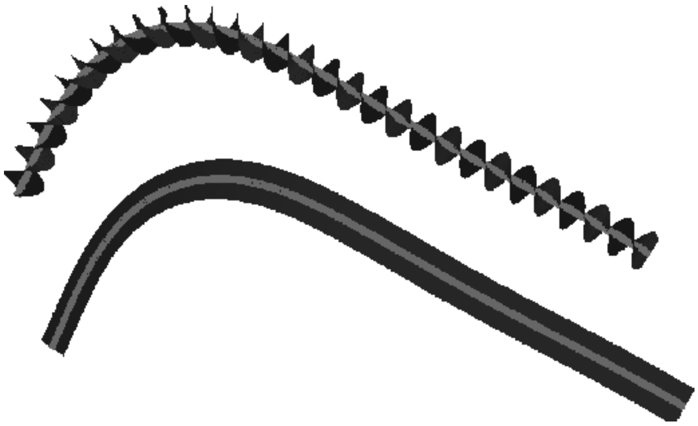

Figure 7.6. A reference configuration with both a high intrinsic twist framing, which models the DNA double helix, and a low intrinsic twist framing.

6. Low twist framings

The role of the directors in a rod theory is to track physical twist. But there is freedom in embedding the directors into the reference configuration of the rod. Figure 7.6 illustrates two framings of a given reference configuration centerline $\hat{\mathbf{r}}$. In this review we are concerned with the case of an inextensible and unshearable rod, so it suffices to consider only *adapted* framings in which the unit vector $\hat{\mathbf{r}}'$ is one of the directors. Any two adapted framings $\{\mathbf{d}_i\}$ and $\{\mathbf{D}_i\}$ are related by a rotation about $\mathbf{d}_3$

through an angle $\Omega(s)$

$$\begin{pmatrix} \mathbf{D}_1^T \\ \mathbf{D}_2^T \\ \mathbf{D}_3^T \end{pmatrix} = \mathbf{R}(\Omega) \begin{pmatrix} \mathbf{d}_1^T \\ \mathbf{d}_2^T \\ \mathbf{d}_3^T \end{pmatrix}, \tag{7.14}$$

where the rotation matrix $\mathbf{R}(\Omega)$ is

$$\mathbf{R}(\Omega) = \begin{pmatrix} \cos\Omega & \sin\Omega & 0 \\ -\sin\Omega & \cos\Omega & 0 \\ 0 & 0 & 1 \end{pmatrix}. \tag{7.15}$$

It is important to note that while the relation between the framings $\{\mathbf{d}_i\}$ and $\{\mathbf{D}_i\}$ encapsulated in equations (7.14) and (7.15) can be set in the reference configuration, the same relation holds in any configuration of the rod. It is merely a change of coordinates.

Just as the frame $\{\mathbf{d}_i\}$ has a strain vector $\mathbf{u}$ defined by (7.1) with components u in the frame $\{\mathbf{d}_i\}$, the frame $\{\mathbf{D}_i\}$ has its own strain vector $\mathbf{U}$ with components U in the frame $\{\mathbf{D}_i\}$. Moreover it is easy to compute that for any angle function $\Omega(s)$

$$U_3(s) = u_3(s) + \Omega'(s) \tag{7.16}$$

in any configuration, and in particular in the reference configuration

$$\hat{U}_3(s) = \hat{u}_3(s) + \Omega'(s). \tag{7.17}$$

The objective is to perform an asymptotic expansion in the high intrinsic twist of DNA. To that end it is important to refer the equilibrium equations to a director frame that is independent of the high twist $\hat{u}_3$. The computations of [22], and the first averaging results [19, 23], adopted the *natural* or parallel transport frame that has no twist in the reference configuration, i.e. $\hat{U}_3(s) \equiv 0$. This condition suffices to fix the angle $\Omega(s)$ via (7.17) and the initial choice $\Omega(0) = 0$. As remarked in [20, 25] it is important in the analysis of the corrector (or first-order) terms in a high twist expansion to make a slightly different choice, namely for a rod of nondimensionalized length one, take

$$\Omega(s) = -2\pi N s, \tag{7.18}$$

with N being the integer part of $\int_0^1 \hat{u}_3(s)\, ds/2\pi$. The integer N will be approximately one tenth of the number of base pairs being modelled by the rod, and

$$\epsilon = \frac{1}{2\pi N} \tag{7.19}$$

will be our small parameter in the limit $N \to \infty$. For the choice (7.18) the frames $\{\mathbf{d}_i\}$ and $\{\mathbf{D}_i\}$ coincide at both $s = 0$ and at $s = 1$.

It remains to write the equilibrium conditions in the $\{\mathbf{D}_i\}$ frame. To that end consider the triple M of the components $M_i = \mathbf{m} \cdot \mathbf{D}_i$ of the moment vector $\mathbf{m}$. The components M in the $\{\mathbf{D}_i\}$ frame are related to the components m in the $\{\mathbf{d}_i\}$ frame via

$$\mathsf{M} = \mathbf{R}(\Omega)\mathsf{m}.$$

The equilibrium equations remain Hamiltonian, but now with

$$H(\mathbf{z}, s, \Omega) = W^*\big(\mathbf{R}^T(\Omega)\mathsf{M}, \mathsf{s}\big) + \mathsf{M} \cdot \hat{\mathsf{U}} + \mathbf{n} \cdot \mathbf{D}_3. \tag{7.20}$$

It is important that Ω enters only through the rotation matrix (7.15), so that the Hamiltonian is always 2π-periodic in Ω, and that the dependence on Ω appears only via the Legendre transform W^* of the strain energy function W. The intrinsic curvature term $\mathsf{M}\cdot\hat{\mathsf{U}}$ has no dependence on Ω.

7. Homogenization in high intrinsic twist

With the choice (7.18) for the angle function Ω, and with the small parameter (7.19), the Hamiltonian (7.20) gives rise to a system of the form

$$\mathbf{z}' = \mathbf{J}\nabla H\left(\mathbf{z}, s, \frac{s}{\epsilon}\right), \tag{7.21}$$

where the dependence on the fast variable s/ϵ is periodic of period 2π. As observed in [19, 23] the hard work is now over provided that the problem at hand involves only initial conditions. For given initial conditions, and in the limit as ϵ tends to zero, standard methods imply that solutions of (7.21) are well approximated by solutions of an effective Hamiltonian system with the averaged Hamiltonian

$$\overline{H}(\mathbf{z}, s) = \frac{1}{2\pi}\int_0^{2\pi} H(\mathbf{z}, s, \Omega)d\Omega \tag{7.22}$$

that is found by integrating over one period with respect to the fast variable Ω.

It remains to consider the explicit form of the averaged Hamiltonian in the case of rods. From (7.20) and (7.22), we find

$$\overline{H}(\mathbf{z}, s) = \overline{W}^*(\mathsf{M}, \mathsf{s}) + \mathsf{M} \cdot \hat{\mathsf{U}} + \mathbf{n} \cdot \mathbf{D}_3,$$

where

$$\overline{W}^*(\mathsf{M}, \mathsf{s}) = \frac{1}{2\pi}\int_0^{2\pi} \mathsf{W}^*(\mathbf{R}^{\mathsf{T}}(\Omega)\mathsf{M}, \mathsf{s})\mathsf{d}\Omega. \tag{7.23}$$

It is important to note that $\overline{W}^*$ is not the Legendre transform of the average of $W(\mathbf{R}^T(\Omega)\mathsf{U},\mathsf{s})$, since the averaging operator and the Legendre transform do not commute. On the other hand, by assumption, $W^*(\mathsf{M},\mathsf{s})$ is a convex function of M, so its average $\overline{W}^*(\mathsf{M},\mathsf{s})$ defined in (7.23) is also convex. Therefore an effective strain energy function $\overline{W}$ can be computed as the Legendre transform of the averaged Legendre transform (7.23). Effectively, the effective model for a high intrinsic twist rod is an effective rod with a convex strain energy density function $\overline{W}$.

For non-quadratic functions W, it does not seem feasible to compute the effective function $\overline{W}$ explicitly. However, Kehrbaum [23] proved an important property of $\overline{W}$, namely it satisfies (7.10), and so is always isotropic. Consequently the effective rod is isotropic precisely if the intrinsic curvatures vanish, i.e. $\hat{U}_1 \equiv \hat{U}_2 \equiv 0$. As previously argued, this property supports the use of the integrable case of the twisted ring solution set as an organizing center for the computation of DNA minicircle configurations via symmetry breaking.

For the specific W given in (7.3), the Legendre transform W^* is given in (7.8), and (7.23) reduces to

$$\overline{W}^*(\mathsf{M},\mathsf{s}) = \frac{1}{2}\bar{\mathsf{K}}(\mathsf{s})^{-1}\left(\mathsf{M}_1^2 + \mathsf{M}_2^2\right) + \frac{1}{2}\mathsf{K}_3(\mathsf{s})^{-1}\mathsf{M}_3^2 \tag{7.24}$$

with the single effective isotropic bending stiffness being given by the harmonic average

$$\bar{K}(s) = \frac{2}{K_1(s)^{-1} + K_2(s)^{-1}},$$

and the associated effective strain energy density function being

$$\overline{W}(\mathsf{U},\mathsf{s}) = \frac{1}{2}\bar{\mathsf{K}}(\mathsf{s})\left(\mathsf{U}_1^2 + \mathsf{U}_2^2\right) + \frac{1}{2}\mathsf{K}_3(\mathsf{s})\mathsf{U}_3^2. \tag{7.25}$$

The modelling of DNA minicircles presented in [22] assumed (7.25) as its starting point.

The effective strain energy density function $\overline{W}$ can be computed explicitly whenever W^* is quadratic. However the closed form expressions are in general formidable. A model for DNA put forward by Marko and Siggia [44] is one tractable, non-diagonal example. They propose

$$W(\mathsf{v},\mathsf{s}) = \frac{1}{2}\sum_{\mathsf{i}=1}^{3}\mathsf{K}_\mathsf{i}(\mathsf{s})\mathsf{v}_\mathsf{i}^2 + \mathsf{K}_{23}(\mathsf{s})\mathsf{v}_2\mathsf{v}_3,$$

with a coupling term between bending and twisting. Following the procedure described above, the effective strain energy density in the high twist limit can be calculated to be

$$\overline{W}(\mathsf{V},\mathsf{s}) = \frac{\bar{\mathsf{K}}_\delta(\mathsf{s})}{2}(\mathsf{V}_1^2 + \mathsf{V}_2^2) + \frac{\mathsf{K}_3(\mathsf{s})(1-\delta)}{2}\mathsf{V}_3^2,$$

where $\delta = K_{23}^2/(K_2 K_3)$ couples the isotropic effective bending stiffness

$$\bar{K}_\delta^{-1} = \frac{1}{2}\left(K_1^{-1} + K_2^{-1}(1-\delta)\right).$$

with the twist rigidity K_3.

8. First-order corrections for high-twist rods

The analysis of [23, 19] provided the first results toward understanding the high twist approximation in elastic rods. However the methods dealt only with initial value problems, while the more natural problem for rods involves two-point boundary conditions. With the introduction of the choices (7.18) and (7.19), Rey [20, 25] was able to extend this work to two-point boundary value problems of an appropriate class. In cases where the effective boundary value problem has locally isolated solutions, typically when there are intrinsic curvatures so that the effective problem is not isotropic, it also followed that any solution of the effective boundary value problem was a limit of high twist solutions as $\epsilon \to 0$.

Cases with no intrinsic curvature, so that the effective rod is isotropic, are more delicate, when, as described in Section 3, the register symmetry generates an orbit of solutions for the effective boundary value problem. Then a Poincaré-Melnikov analysis (as described in Section 4) is again required, and can still be forced through for the two-scale expansion, in order to determine which solutions persist for high, but finite intrinsic twists.

Figure 7.7 illustrates a numerical experiment described in [20, 25]. A uniform rod with strain energy density function of the form (7.3), and intrinsic shape parameters $\hat{u}_1 \equiv \hat{u}_2 \equiv 0$, $\hat{u}_3 \equiv \tau$, is subject to *clamped-free strut* boundary conditions, i.e. the lower end is vertically clamped, while the upper end is loaded by a vertical force of magnitude λ. The effective rod is isotropic, and can buckle in any vertical plane. However, the Poincaré function analysis for this example predicts that high twist solutions can only approach those buckled equilibria of the effective rod lying in the two vertical planes making a 45° angle with the principal planes at $s = 0$. Remarkably enough, this result is independent of the values of the stiffnesses K_1, K_2, K_3, and of the load λ. The prediction is compatible with the numerical computations shown in Figure 7.7, and the convergence is seen to be quite rapid. When $\tau = 0$, the rod buckles in

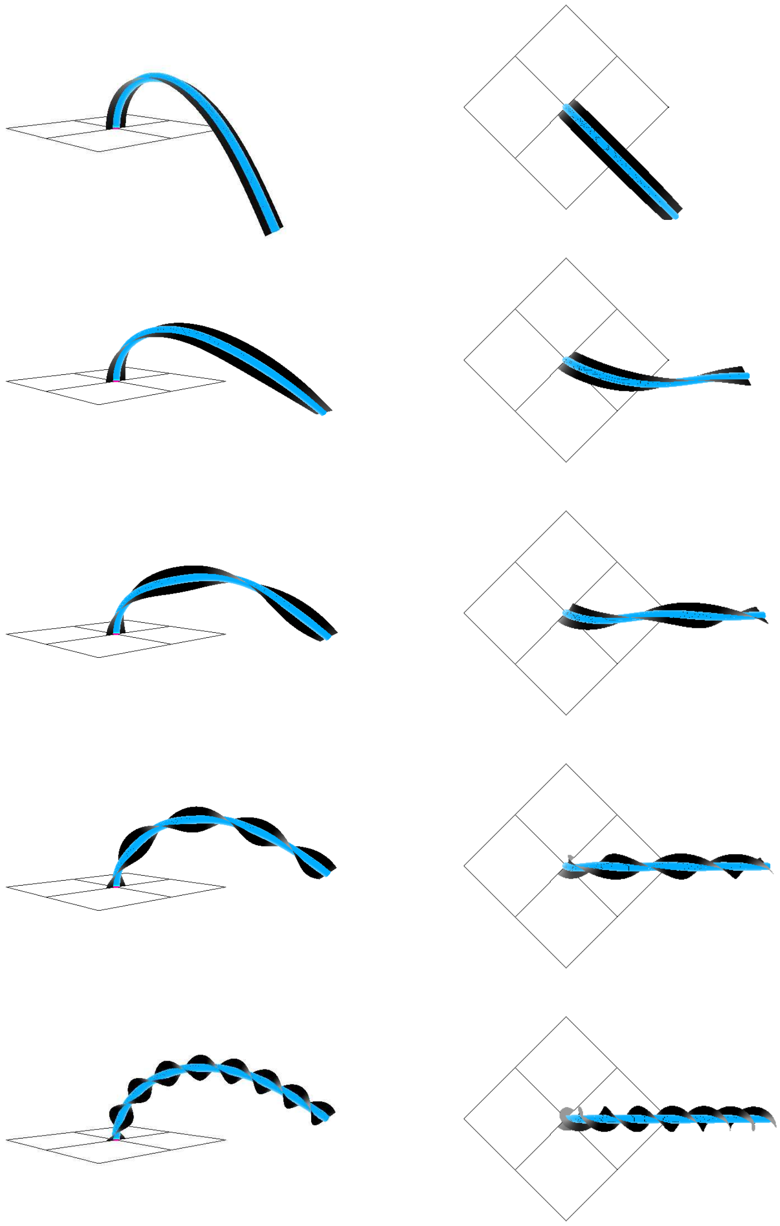

Figure 7.7. *For different values of the intrinsic twist τ, side (left) and top (right) views of a buckled configuration of a clamped-free strut with stiffness constants $K_1 = 0.1$, $K_2 = 0.4$, $K_3 = 0.4$, and load $\lambda = 0.75$.*

its soft plane at the clamped end. When $\tau \neq 0$, the buckled configuration is no longer planar. However, as τ increases, the equilibrium rapidly approaches a 45° plane.

Yet another behaviour is possible. The choice (7.19) relates ϵ to an integer number of turns, i.e. $\epsilon = \epsilon_N$. There exist examples in which a) the effective problem has a loop of nonisolated equilibria, b) as $N \to \infty$ the sequence $\mathbf{z}(\epsilon_N)$ of solutions to the boundary value problem approaches a given solution of the effective problem, but c) as $\epsilon \to 0$ through the real numbers, the high twist solutions spiral ever faster around the entire orbit of effective solutions.

9. Afterword

The work surveyed in this article was carried out over a number of years in both the Laboratory for Computation and Visualization in Mechanics (or $LCVM$) in College Park and in the Laboratory for Computation and Visualization in Mathematics and Mechanics (or $LCVM^2$) in Lausanne. It was largely, and generously, supported by the US Air Force Office of Scientific Research, the US National Science Foundation, and the Swiss National Science Foundation. In addition to the authors of the cited articles and theses, all of the group members over the years contributed greatly, and it is a pleasure for me to be able to thank them all–they know who they are.

I should also like to relate a final anecdote. In the Autumn of 2000 JBK and Alice Whittemore visited me in Lausanne. During that visit JBK was instrumental both in encouraging Stéphane Rey to pursue a thesis which lent rigor to, and extended what had gone before in the work of my group on modelling DNA, and in suggesting mathematical ways to proceed. The culmination of those suggestions was the thesis [20] which figures prominently in this review.

During the same visit I arranged an excursion to the top of a nearby alp, of height some two thousand and more meters. I realized my first mistake when it became clear that Joe would have preferred to have walked up rather than take the cog railway as I had arranged. We compromised and walked down. During the descent of the somewhat nontrivial alpine path, I remember contemplating my potential second mistake, and wondering whether my own place in the history of applied mathematics would be to be known as the person who led Joe to fall off a Swiss mountain. Fortunately that did not transpire, so that I have the opportunity to thank Joe, on behalf of myself and many others, for helping to start us on our mountain paths across the mathematical landscape.

References

[1] Watson J.D. and Crick F.H.C., "A Structure for Deoxyribonucleic Acid", Nature, **171** 737-8, 1953

[2] Watson J.D. *The Double Helix*, Norton Critical Edition, Ed. Gunther S. Stent, New York and London, W.W. Norton and Company, 1980

[3] Maddox, Brenda, *Rosalind Franklin: The Dark Lady of DNA*, New York, HarperCollins, 2002

[4] Vologodskii, A. *Topology and Physics of Circular DNA*, Boca Raton, CRC Press, 1992

[5] Stasiak, A. "Circular DNA", in *Large Ring Molecules*, Ed. J.A. Semlyen, Chichester, John Wiley & Sons, 1996

[6] Călugăreanu, G. "L'Intégrale De Gauss et L'analyse des Noeuds Tridimensionnels," R. de Math. Pures and Appliquees, **4**, 5-20, 1959

[7] Călugăreanu, G. "Sur les Classes D'Isotopie des Noeuds Tridimensionnels et Leurs Invariants," Czech. Math. J., **11**, 588-625, 1961

[8] Fuller, Brock F., "The Writhing Number of a Space Curve", PNAS USA, **68** , **#4**, 815-819, 1971

[9] Fuller, Brock F., "Decomposition of the Linking Number of a Closed Ribbon: A Problem from Molecular Biology", PNAS USA, **75**, **#8**, 3557-3561, 1978

[10] White, J. H.,"Self-Linking and the Gauss Integral in Higher Dimensions", Amer. J. Math., **91** , 963-728, 1969

[11] White, J. H. and Bauer, W. R., "Calculation of the Twist and the Writhe for Representative Models of DNA", J. Mol. Biol., **189** , 329-341, 1986

[12] Voet, D. and Voet, J.G. *Biochemistry* 2nd Ed. New York, John Wiley & Sons, 1995

[13] Various authors in Special Issues, Science, April 11, 2003, and Nature, April 24, 2003.

[14] Keller, Joseph B.,"Semiclassical Mechanics", SIAM Review, **27**, 485-504, 1985

[15] Keller, Joseph B., and Rubinow S.I., "Slender-Body Theory for Slow Viscous Flow", J. Fluid Mech. **75**, 705-714, 1976

[16] Keller, Joseph B., and Rubinow S.I., "Swimming of Flagellated Microorganisms", Biophys. J., **16** , 151-170, 1976

[17] Mohanty, Udayan, and Taubes, Clifford Henry, "Dynamics of Bent Molecules in Gels" J. Phys. Chem. B, **107**, 6187-6193, 2003

[18] Manning R.S. and Maddocks J.H., "Symmetry breaking and the twisted elastic ring", Comp. Meth. Appl. Mech. Eng. **170**, 313-330, 1999

[19] Kehrbaum S. and Maddocks J.H., "Effective properties of elastic rods with high intrinsic twist", Proc. 16th IMACS World Congress, Lausanne, 2000

[20] Rey S., *Symmetry Breaking, Averaging and Elastic Rods with High Intrinsic Twist*, Ph. D. Thesis, EPF–Lausanne, 2002

[21] Dichmann D.J., Li Y. and Maddocks J.H., "Hamiltonian formulations and symmetries in rod mechanics", in *Mathematical Approaches to Biomolecular Structure and Dynamics*, The IMA Volumes in Mathematics and its Applications **82** , 71-113, 1996

[22] Manning R.S., Maddocks J.H. and Kahn J.D., "A continuum rod model of sequence-dependent DNA structure", J. Chem. Phys. **105**, 5626-5646, 1996

[23] Kehrbaum S., *Hamiltonian Formulations of the Equilibrium Conditions Governing Elastic Rods: Qualitative Analysis and Effective Properties*, Ph.D. Thesis, University of Maryland, 1997

[24] Kehrbaum S. and Maddocks J.H., "Elastic rods, rigid bodies, quaternions and the last quadrature", Phil. Trans. R. Soc. Lond. A **355**, 2117-2136, 1997

[25] Rey S. and Maddocks J.H., "Buckling of an Elastic Rod with High Intrinsic Twist", Proc. 16th IMACS World Cong. Lausanne, 2000

[26] Furrer P.B., Manning R.S. and Maddocks J.H., "DNA Rings with Multiple Energy Minima", Biophysical J. **79**, 116-136, 2000

[27] Calladine C.R. and Drew H.R. *Understanding DNA: The molecule and how it works* 2nd Ed. London, Academic Press, 1997

[28] Bednar J., Furrer P., Katritch V., Stasiak A.Z., Dubochet J. and Stasiak A. "Determination of DNA Persistence Length by Cryo-Electron Microscopy. Separation of the Static and Dynamic Contributions to the Apparent Persistence Length of DNA", J. Mol. Biol. **254**, 579-594, 1995

[29] Dustin I., Furrer P., Stasiak A., Dubochet J., Langowski J. and Egelman, E., "Spatial Visualization of DNA in Solution", J. of Structural Biol., **107**, 15 - 21, 1991

[30] Bednar J., Furrer P., Stasiak A., Dubochet J., Egelman E. H. and Bates A. D., "The twist, writhe and overall shape of supercoiled DNA change during counterion-induced transition from a loosely to a tightly interwound superhelix. Possible implications for DNA structure in vivo", J. Mol. Biol. **235**, 825-847 , 1994

[31] Zhang, Yongli, and Crothers, Donald M. "Statistical Mechanics of Sequence-Dependent Circular DNA and Its Application For DNA Cyclization", Biophysical J. **84**, 136-153, 2003

[32] Olson W.K., Gorin A.A, Lu X.J., Hock L.M. and Zhurkin V.B., "DNA sequence-dependent deformability deduced from protein-DNA crystal complexes", PNAS USA **95**, 11163-11168, 1998

[33] Lankas F., Sponer J., Hobza P. and Langowski J. "Sequence-dependent elastic properties of DNA" J. Mol. Biol. **299**, 695-709, 2000

[34] Lankas F., Sponer J., Langowski J. and Cheatham III, T.E. " DNA base-pair step deformability inferred from molecular dynamics simulations" Biophysical J., in press

[35] Scipioni A., Anselmi C., Zuccheri G., Samori B. and DeSantis P. "Sequence-dependent DNA curvature and flexibility from scanning force microscopy images" Biophysical J. **83**, 2408-2418, 2002

[36] Gonzalez O. and Maddocks J.H., "Extracting parameters for base-pair level models of DNA from molecular dynamics simulations", Theoretical Chemistry Accounts **106**, 76-82, 2001.

[37] Antman S.S., *Nonlinear Problems of Elasticity*, New York, Springer-Verlag, 1995

[38] Michell, J.H., "On the stability of a bent and twisted wire," Messenger of Math. **11**, 181-184, 1889-90

[39] Zajac, E.E., "Stability of two planar loop elasticas" ASME J. Applied Mech. 136-142, March, 1962

[40] Le Bret M. "Catastrophic Variation of Twist and Writhing of Circular DNAs with Constraint?", Biopolymers, **18** , 1709-1725, 1979

[41] Benham, C.J., "Geometry and Mechanics of DNA Superhelicity", Biopolymers, **22**, 2477-2495, 1983

[42] Stuart, C.A. "Bifurcation of homoclinic orbits and bifurcation from the essential spectrum", SIAM J. Math. Anal. **20** , 1145-1171, 1989

[43] Ambrosetti, A. and Badiale, M., "Homoclinics: Poincaré-Melnikov type results via a variational approach", Ann. Inst. Henri Poincaré **15** , 233-252, 1998

[44] Marko, J.F. and Siggia, E.D. "Bending and Twisting Elasticity of DNA", Macromolecules, **27**, 981-988, 1994